THE AMERICAN SOCIETY OF MECHANICAL ENGINEERS
345 E. 47th St., New York, N.Y. 10017

97-GT-501

An Experimental Investigation of Vibration Localization in Bladed Disks, Part I: Free Response

Marlin J. Kruse and Christophe Pierre

University of Michigan
Mechanical Engineering and Applied Mechanics
Ann Arbor, MI U.S.A.

ABSTRACT

The results of an experimental investigation of the effects of random blade mistuning on the free dynamic response of bladed disks are reported. Two experimental specimens are considered: a nominally periodic twelve-bladed disk with equal blade lengths, and the corresponding mistuned bladed disk, which features slightly different, random blade lengths. In the experiment, both the spatially extended modes of the tuned system and the localized modes of the mistuned system are identified. Particular emphasis is placed on the transition to localized mode shapes as the modal density in various frequency regions increases. Excellent qualitative and quantitative agreement is obtained between experimental measurements and results obtained by finite element analysis. Experimental results are additionally used to validate a component mode-based, reduced-order modeling technique for bladed disks. This work reports the first systematic experiment carried out to demonstrate the occurrence of vibration localization in bladed disks.

1. INTRODUCTION

Cyclic structures, such as bladed disks, are assumed to be made of identical substructures, or sectors. In addition to describing the geometry of the entire structure, a fundamental sector also determines its dynamic behavior. Modern structural analysis of bladed disks is greatly simplified by this observation. The assumption of cyclic symmetry enables engineers to create highly detailed finite element models of a single sector in order to examine the dynamic response of the entire blade assembly. However, cyclic symmetry implies that all sectors are identical, that is, that the bladed disk is tuned. Unfortunately, small differences in the structural properties of individual blades, due to manufacturing and material tolerances, or in-service degradation, often destroy any symmetry. These irregularities, which are referred to as blade mistuning, may lead to qualitatively different dynamic behavior than that experienced by a perfectly tuned assembly. Namely, irregularities may inhibit the propagation of vibrations within the structure and confine vibrational energy to a few, or even a single blade. Mode shapes may become spatially localized and, as a result, a single blade could experience deflections much larger than that predicted by a tuned analysis.

To date, three of the most thorough experimental investigations of bladed disk dynamics were carried out by Ewins (1969,1973,1976) in the 1970's, and by Irretier (1983) and Fabunmi (1980) in the early 1980's. Ewins fabricated a nominally tuned 24-bladed disk by machining the disk and blades from a single piece of material. Individual blades could be detuned in a known and controlled manner by the addition of shims to the tips of each blade. Ewins (1973) observed the formation of what he called complex modes of vibration. At the time, these modes could not be explained and their description in his paper was relegated to an appendix. The complex modes that Ewins observed would later become known as localized modes. Both Irretier (1983) and Fabunmi (1980) observed departure from perfectly tuned modes shapes, but were unable to explain mode localization or predict the formation and severity of localized modes with either finite element or component mode analysis techniques.

It was not until 1988, when Wei and Pierre (1988a, 1988b) examined the free and forced response of bladed disks, that an appreciation for mode localization was achieved. Wei and Pierre (1988a) documented the existence of localized modes in mistuned bladed disks through the investigation of a single-degree of freedom per sector model. They determined that the sensitivity of bladed disks to mistuning depends primarily upon the ratio of mistuning strength to coupling strength. Considering the realistic case of small mistuning, they found that mistuning has a relatively small effect on the free response of bladed disks that exhibit strong interblade coupling. However, for weak interblade coupling, mistuning dramatically localizes what were once spatially extended mode shapes. In addition to investigating localized modes computationally, Wei and Pierre also proposed a perturbation formulation to a general eigenvalue problem and found that, to first order, the eigenvector perturbation is inversely proportional to the difference in eigenvalues. Structures with high modal densities, they concluded, are more susceptible to mode localization than structures with widely spaced eigenvalues. As

Presented at the International Gas Turbine & Aeroengine Congress & Exhibition
Orlando, Florida — June 2–June 5, 1997

we shall see later, bladed disks exhibit extremely high modal densities in frequency regions where the mode shapes of the structure are dominated by cantilever blade motion.

Although significant, Wei and Pierre's contributions were limited to very simple, single-degree of freedom models of bladed disks. Lumped mass models of bladed disks capture the basic dynamics of the assembly, but are difficult to relate to more descriptive finite element models. By necessity, finite element models of industrial turbomachinery rotors assume perfect periodicity in the structure and use cyclic symmetry analysis routines to reduce the computational size and cost of the problem. Full mistuned finite element analyses are simply not practical—see Kruse and Pierre (1996a). However, as Ewins (1969,1973,1976) and Wei and Pierre (1988a,1988b) pointed out, small inherent differences in the structural properties of individual blades can affect dynamic behavior drastically and thus cannot be ignored.

In 1994, Ottarsson *et al.* (1994) and Kruse and Pierre (1996b) made a significant contribution to mistuned bladed disk analysis when they introduced a technique for developing reduced-order models (ROMs) of bladed disks directly, and systematically, from finite element models. The procedure involves a component mode analysis of the bladed disk, with a truncated number of modal amplitudes describing the response of the assembly. The key idea introduced by Ottarsson *et al.* (1994) is that the motion of an individual blade consists of cantilever blade elastic motion and disk-induced static motion. The principal advantage of the technique is the tremendous computational savings associated with solving a full mistuned rotor model with a reduced set of degrees of freedom—see Kruse and Pierre (1996a). One objective of this paper is to demonstrate the correlation between experimental, finite element, and ROM free response predictions for general bladed disk assemblies.

This paper presents an experimental investigation of the effect of blade mistuning on the free response of bladed disks. The primary objective of the paper is to verify the existence of localized modes in bladed disk assemblies. However, experimental results are also used to validate both finite element and reduced-order modeling techniques. Section 2 describes the experimental apparatus and procedure. Natural frequencies and spatially extended mode shapes of the tuned experimental bladed disk are examined in Section 3. In Section 4, the effect of modal density and manufacturing tolerances on the tuned specimen's mode shapes is examined. Natural frequencies and mode shapes for the mistuned experimental specimen are examined in Section 5, particular attention being paid to the formation of localized modes. There are three main contributions of this work. First, the work reports the first systematic experiment carried out to demonstrate the occurrence of vibration localization in bladed disks. Second, the paper thoroughly documents the formation of spatially localized mode shapes from extended modes as the modal density of the structure increases. Third, the paper demonstrates that component mode-based, reduced-order models can accurately predict the formation of localized modes. The validation of the reduced-order modeling technique is of particular importance to the industrial manufacturers of turbomachinery rotors, since statistical, or even single mistuning pattern, analyses with finite element models are computationally prohibitive for most industrial rotor designs.

2. THE EXPERIMENTAL APPARATUS AND PROCEDURE

The dynamics of engineering structures are typically studied experimentally by identifying the natural frequencies and mode shapes of the structure. Mode shapes are generally obtained using modal analysis packages that process the measured acceleration, velocity, or displacement of selected points on the structure. However, periodic structures, such as bladed disks, are difficult to analyze using modal software due to their characteristic high modal densities. We, therefore, choose to obtain the mode shapes and natural frequencies of the bladed disks by examining the resonant forced responses of the structure to single blade excitations. Assuming small damping, which is valid for the experimental specimens at hand, the forced response of the blade assembly is dominated by its individual modes at the resonances. The mode shapes of the structure, therefore, can be obtained by measuring the blade tip displacement of each blade at the resonant frequencies.

Experimental Setup

In order to highlight the effect of mistuning on the free response of the rotor, and prevent contamination by unwanted rotational effects (e.g., aerodynamic and centrifugal effects), the bladed disk was held stationary, as shown in Fig. 1. A 20-ton capacity bearing press held the disk stationary through the spindle connection shown in Fig. 2. Tight diametral tolerances (0.0254 mm, 0.001 inches) between the center hole in the disk and the spindles were maintained to ensure precision centering of the disk and symmetrical boundary conditions.

In addition to holding the disk stationary, it was also desirable to minimize any additional mistuning associated with the excitation and the displacement measurement techniques. Electromagnets, therefore, were chosen to provide the excitation force, and a non-contacting Bentley Nevada^{TM} proximity probe measured the displacement of each blade. As shown in Fig. 1-b and 1-c, the magnets and proximity probe could be rotated to excite and measure blade displacements both in and out of the plane of the disk.

Although electro-magnetic excitation has the advantage of being non-contacting, it can lead to super harmonic, as well as, harmonic response. *First*, magnets generate an attraction force whether the current is flowing in the positive or negative directions. A diode circuit was constructed to send only the positive portion of the reference signal to the top magnet, and the negative portion of the reference signal to the bottom magnet, as shown in Fig. 3. *Second*, the force generated by a magnet varies inversely with the cube of the distance between the magnet and the blade. To minimize this nonlinearity, a reasonably large air gap, in comparison to blade deflection, should be maintained at all times. This can become particularly difficult when examining higher frequency modes that require larger excitation forces and necessitate small air gaps.

Clearly, it is not easy to produce pure harmonic excitation with magnets. However, the magnitude of super harmonic response can be minimized. Super harmonic response was observed in the free response experiments, but occurred in very limited frequency regions that were not of particular interest. Its occurrence was detected by monitoring both the reference signal and the response signal on an oscilloscope at the same time. Other sources of excitation, such as piezo-electric actuators, produce purer harmonic excitation than magnets. However, piezo-electric actuators must be bonded to the surface of the blades and, thereby, introduce incidental mistuning. The overriding reason for using magnets to generate the excitation force in the free response experiment is to minimize incidental mistuning.

As mentioned earlier, a non-contacting proximity probe was used to measure blade displacements. A bracket, centered on the top disk spindle, was free to rotate and allowed measurements to be taken at all blades by simply rotating the probe and bracket circumferentially. Since the de-

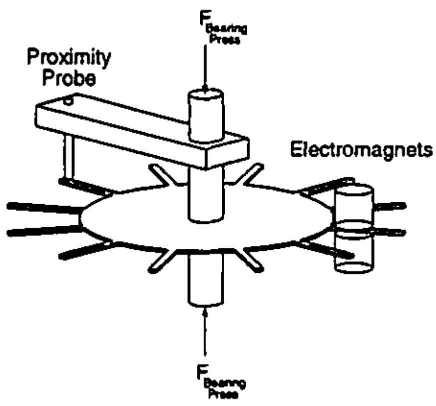

(a)

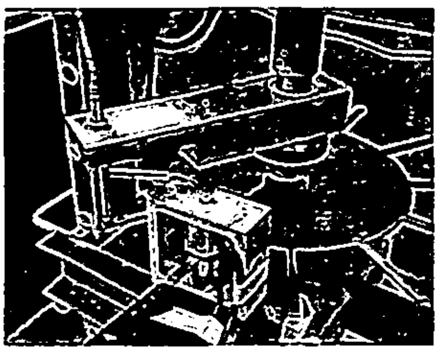

(b)

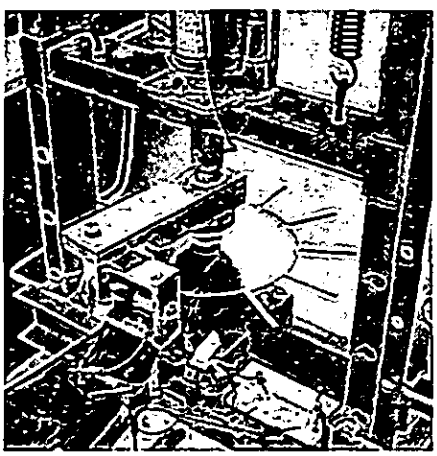

(c)

Fig. 1 Schematic (a) and photographs of out-of-plane (b) and in-plane (c) experimental setups.

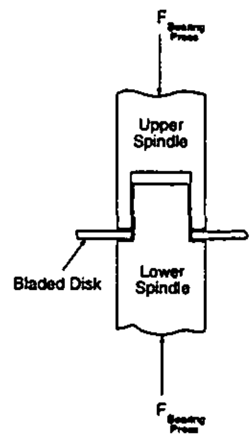

Fig. 2 Section view of the bladed disk-spindle connection.

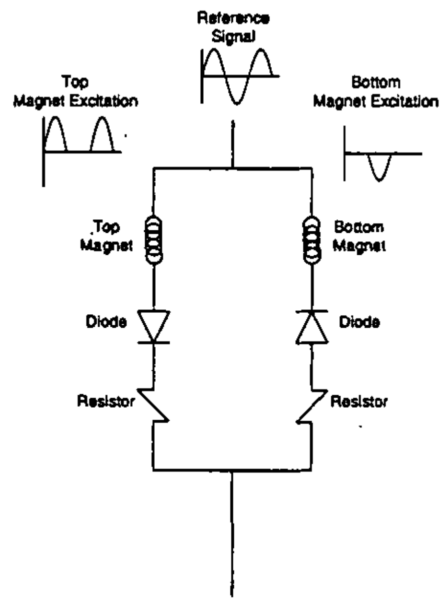

Fig. 3 Diode circuit used to block negative and positive current flows into the top and bottom magnets, respectively.

flection of the blades varies as the cube of the length of the blade, small variations in the radial position of the probe along the blade could lead to large variations in the displacement measurement. To ensure blade-to-blade consistency and repeatability of the measurements, the bracket was used to keep the probe a constant radial distance form the center of the hub. Measurement repeatability also improved when a spacing collar, shown in Fig. 1-b, was added to raise and lower the proximity probe normally to the plane of the disk. The spacer, along with precision shim stock, ensured that a consistent gap was maintained between the proximity probe and each individual blade. Repeatability of the displacement measurements varied from ±2.5% for out-of-plane measurements to ±5% for the in-plane measurements.

Bladed Disk Design and Manufacturing Considerations

Two experimental specimens were manufactured: a nominally periodic twelve-bladed disk with equal blade lengths, and the corresponding mistuned bladed disk which features slightly random blade lengths.

Table 1 **Blade lengths (mm) for the mistuned-bladed disk.**

Blade Number	Mistuned Blade Length
1	92.01
2	93.83
3	94.01
4	93.27
5	91.82
6	91.68
7	91.60
8	91.06
9	92.43
10	92.46
11	92.07
12	90.55

Table 2 Bladed disk material properties.

Material Property	Property Value
Modulus of Elasticity, E_o	$200\ GPa$
Modulus of Rigidity, G	$80\ GPa$
Density, ρ	$7.86\ Mg/m^3$
Structural Damping, G_{Struc}	0.004

The nominal blade length for the tuned test specimen is 92 mm (3.622 inches). Random blade lengths for the mistuned specimen are listed in Table 1. The random lengths are from a uniform probability distribution with stiffness mistuning of 4% standard deviation. For both specimens, the disks are 300 mm (11.811 inches) in diameter and 3.25 mm (0.128 inches) in thickness, with a mounting hole of diameter 25.4 mm (1.000 inch) at the center. In order to minimize mistuning associated with the attachment of individual blades to the disk, the blades and disk were manufactured from a single piece of material. *First*, precision ground 4140 steel plate was purchased. The plate was ground to a thickness of 3.25 mm (0.128 inches) with a tolerance of ± 0.0254 mm (± 0.001 inches). Since the plate was held in a magnetic chuck, the flatness of the plate varied by 0.381 mm (0.015 inches), due to spring back of the material once released from the chuck. Hence, there was a need for a spacing collar to precisely raise and lower the proximity probe normally to the plane of the disk so as to maintain a consistent gap between the probe and individual blades. *Second*, blade profiles and the center disk mounting hole were fabricated using wire electrical discharge machining (EDM) techniques. Tolerances on blade length and width dimensions were held to a nominal ± 0.0254 mm (± 0.001 inches). The tolerances stated above are standard in most machining processes.

Finite Element and Reduced-Order Models

Two theoretical models of the tuned and mistuned experimental blisk specimens were developed. The *first* model is a detailed finite element representation of the blisk and spindles. Cyclic symmetry routines in MSC/NASTRAN^{TM} were used to calculate the natural frequencies and mode shapes of the tuned finite element model. Material properties for the finite element model are listed in Table 2. The disk and spindle portion of the cyclic symmetry model consists of 162 six-noded wedge and eight-noded brick elements. The number of wedge elements was kept to a minimum, and these were only used in mesh transitional areas. The blade portion of the model uses eight eight-noded brick elements. The spindles are constrained in all degrees of freedom at the junction between the spindles and the bearing press. The disk-spindle connection is modeled as one continuous piece of material. No effort was made to use constraint equations to model the disk-spindle connection in a manner consistent with bolted joints. The mistuned finite element model consists of an entire assembly of blades. The same mesh pattern is used in both the single sector cyclic symmetry model and the full mistuned finite element model. Mistuning is introduced to the full finite element model by allowing each blade to have a random blade length, as specified in Table 1. There is a total of 9,042 degrees of freedom in the mistuned finite element model.

The *second* model is a reduced-order model (ROM) (Ottarsson et al., 1994; Kruse and Pierre, 1996b), which is derived systematically from the finite element representation using component mode synthesis techniques. Although the ROM is slightly less accurate than the finite element model, it features only 120 degrees of freedom, as opposed to the 9,042 degrees of freedom of the mistuned finite element model. The ROM consists of five disk-induced modes and five cantilever blade modes per sector, for a total of 120 degrees of freedom.

3. SPATIALLY EXTENDED MODE SHAPES OF THE TUNED SPECIMEN

A convenient method to describe the mode shapes of bladed disks is in terms of nodal diameters and nodal circles. Nodal diameters are nodal lines across the diameter of the disk, while nodal circles are nodal lines in the circumferential direction. Information about the nodal diameter and nodal circle characteristics of a mode are conveniently summarized by a plot of natural frequencies versus the number of nodal diameters, as shown in Fig. 4.

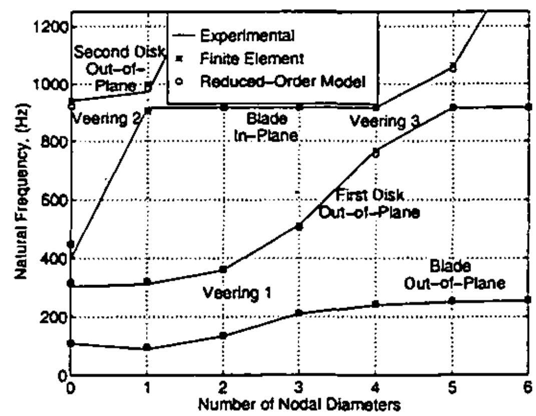

Fig. 4 Tuned natural frequencies versus number of nodal diameters. Note the excellent agreement between experimental, finite element, and ROM natural frequencies.

Figure 4 displays the natural frequencies of the tuned blisk, as obtained from experimental measurements, finite element analysis, and ROM analysis. Natural frequencies below 800 Hz and above 950 Hz

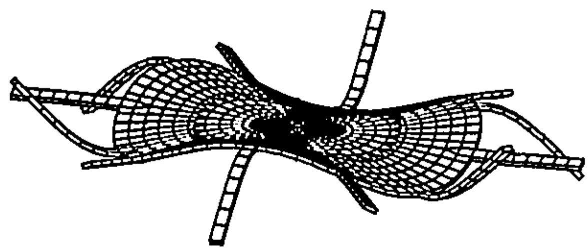

Fig. 5 Tuned three nodal diameter mode at 514 Hz. Disk-induced and cantilever blade motion dominate this mode shape.

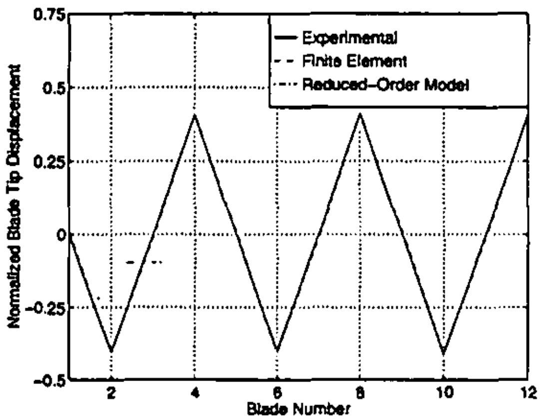

Fig. 6 Comparison of experimental, finite element, and ROM three nodal diameter tuned mode shapes at 514 Hz.

are associated with mode shapes in which the disk and blade deflect normally to the plane of the disk—the so-called out-of-plane modes. The family of modes at 917 Hz is characterized by in-plane blade motion. In general, finite element and ROM natural frequencies correlate very well to the experimentally determined natural frequencies. Table 3 lists experimental, finite element, and ROM natural frequencies along with the percent discrepancy in parenthesis. Only one finite element and ROM natural frequency, that associated with the zero nodal diameter in-plane mode shape at 400 Hz, does not correlate well to the experimental measurement. The natural frequency of this mode falls from the nominal value of the in-plane blade modes, 917 Hz, to 400 Hz, due to the torsional flexibility associated with the spindle connection. Finite element and ROM natural frequencies for this zero nodal diameter mode are 13% higher than the experimental measurement.

Plotting the natural frequency versus the number of nodal diameters for the blisk specimen in Fig. 1 reveals several interesting features. *First*, as the number of nodal diameters increases, the disk becomes stiffer rapidly. Thus, the slanted lines in Fig. 4 correspond to disk-dominated modes. An example of a three nodal diameter disk mode is illustrated in Fig. 5. The reader should attempt to draw the nodal lines across the diameter of the disk by looking for sets of opposed blades that are pitched, but have nominally zero deflection normal to the plane of the disk. A corresponding plot of blade tip displacement is shown in Fig. 6. Excellent correlation is obtained between experimental, finite element, and

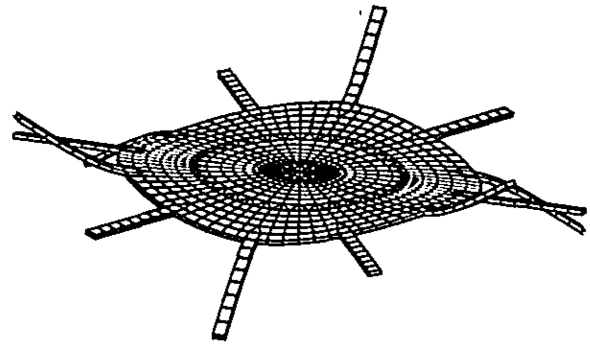

Fig. 7 Tuned three nodal diameter mode at 210 Hz. Cantilever blade motion dominates this mode shape.

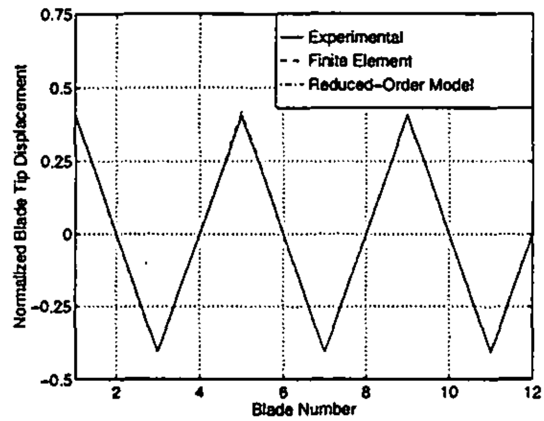

Fig. 8 Comparison of experimental, finite element, and ROM three nodal diameter tuned mode shapes at 210 Hz.

ROM mode shapes. In the absence of blade tip or mid-span shrouding, the number of nodal diameters does not significantly stiffen blade-dominated modes. Lines in Fig. 4 that are approximately horizontal, therefore, represent families of blade-dominated modes. An example of a three nodal diameter blade-dominated mode is illustrated in Fig. 7. A corresponding plot of blade tip displacement is shown in Fig. 8. Again, excellent correlation is obtained between the experimental, finite element, and ROM mode shapes. The modes shapes in Figs. 5-8 were selected not only because of the excellent correlation between experimental and computational modes, but also because they illustrate the fundamental disk-induced and cantilever blade motions that are used as the component modes of the reduced-order modeling technique.

Second, in Fig. 4 there are three areas, called eigenvalue veerings, in which blade and disk families of modes veer away from each other. Physically, eigenvalue veerings are indicative of the degree of coupling between families of disk and blade modes. The strength of the veering is measured by the distance between the natural frequencies and the local curvature in the veering region (Pierre, 1988). If coupling is weak, then the loci abruptly veer away from each other. Conversely, strong coupling between modes is characterized by small curvature. Thus, the general appearance of the veerings in Fig. 4 can qualitatively indicate the level of modal interblade coupling through the disk. We expand upon the significance of eigenvalue veerings in the companion paper by Kruse and Pierre (1997), where the effect of interblade coupling on the forced response of the rotor is discussed.

The modes illustrated thus far have one property in common, namely that their natural frequency lies in a region of very low modal density. For example, the nearest neighboring natural frequencies for the three nodal diameter mode at 514 Hz, excluding the repeated root, is nearly 117 Hz away. Yet, the fifth and sixth nodal diameter modes at 252 and 255 Hz, and the zero and one nodal diameter modes at 305 and 313 Hz, are much more densely packed. Modal density increases even further for the in-plane blade modes at 917 Hz, where there is virtually no separation between several natural frequencies. In Sections 4 and 5, the impact of modal density on the mode shapes of mistuned bladed disks is discussed.

4. MANUFACTURING TOLERANCES AND MODAL DENSITY

The nodal diameter description of the modes assumes that the mode shapes of the rotor are themselves cyclic, that is, spatially extended. This is true for tuned bladed disks; however, small blade mistuning may alter the mode shapes and cause the concentration of vibrational energy to a few, or even a single blade—the so-called phenomenon of localization. The observation that the first order mode shape perturbation due to mistuning is inversely proportional to the difference in the tuned system's natural frequencies, leads to the well-known property that the localization of the mode shapes is most acute in frequency regions of high modal density (Pierre, 1988).

Figure 4 suggests that we define three categories of modal density. *First*, disk-dominated modes, which are well spaced from other modes, can be categorized as featuring very low modal density. This suggests that mistuning will have a negligible effect on the nodal diameter description of disk-dominated modes—see Fig. 12 in Section 5. *Second*, out-of-plane blade modes, which feature neighboring natural frequencies that are closer together than for the disk-dominated modes, can be categorized as moderate modal density modes, and are more sensitive to mistuning effects than disk-dominated modes—see Fig. 14.

There is a dramatic increase, however, in modal density for the in-plane blade modes at about 917 Hz. These modes comprise the *third* category of modal density and are extremely sensitive to mistuning effects. Indeed, Fig. 9 illustrates an experimentally measured in-plane blade mode from the nominally tuned test specimen. The mode shape clearly does not match any nodal diameter description and cannot be compared to tuned finite element or ROM mode shapes.

It is important from a design standpoint to verify that the finite element and ROMs are sensitive to such small variations in the structural properties of the bladed disk. Two finite element models were created with the random blade length patterns listed in Table 4. The blade lengths in the column labeled "Slightly Mistuned Blade Lengths" roughly correspond to ± 0.00254 mm (± 0.0001 inches) tolerances. The blade lengths in the column labeled "Fully Mistuned Blade Lengths" are identical to the blade lengths used the mistuned test specimen (see Table 1) and are believed to be more representative of mistuning in actual turbomachinery rotors. Figure 10 illustrates the gradual degradation, as determined by finite element modeling, in the nodal diameter description with an increase in the level of mistuning, for an in-plane, three-nodal diameter blade mode. Note that intermediate mistuning strengths, not presented in Fig. 10, were analyzed in order to track the three nodal diameter mode. The choice of a three nodal diameter mode for the finite element analysis is completely arbitrary, since the experimentally measured modes in

Table 3 Comparison of experimental, finite element, and ROM tuned natural frequencies (Hz).

Mode Number	Experimental	Finite Element	Reduced-Order Model
1	88.8	96.3 (+8.4%)	96.6 (+8.8%)
2	88.8	96.3 (+8.4%)	96.6 (+8.8%)
3	110.4	112.2 (+1.6%)	111.5 (+1.0%)
4	133.9	135.3 (+1.0%)	135.9 (+1.5%)
5	133.9	135.3 (+1.0%)	135.9 (+1.5%)
6	209.6	210.3 (+0.3%)	212.2 (+1.2%)
7	209.6	210.3 (+0.3%)	212.2 (+1.2%)
8	240.3	242.3 (+0.8%)	244.9 (+1.9%)
9	240.3	242.3 (+0.8%)	244.9 (+1.9%)
10	251.6	254.0 (+1.0%)	256.5 (+1.9%)
11	251.6	254.0 (+1.0%)	256.5 (+1.9%)
12	254.9	257.1 (+0.9%)	257.8 (+1.1%)
13	304.5	315.8 (+3.7%)	317.5 (+4.3%)
14	312.5	319.3 (+2.2%)	324.0 (+3.7%)
15	312.5	319.3 (+2.2%)	324.0 (+3.7%)
16	359.6	363.0 (+0.9%)	361.8 (+0.6%)
17	359.6	363.0 (+0.9%)	361.8 (+0.6%)
18	396.8	448.7 (+13.1%)	449.1 (+13.2%)
19	513.9	510.5 (-0.7%)	504.6 (-1.8%)
20	513.9	510.5 (-0.7%)	504.6 (-1.8%)
21	768.4	765.8 (-0.3%)	755.0 (-1.7%)
22	768.4	765.8 (-0.3%)	755.0 (-1.7%)
23	917.0	905.0 (-1.3%)	907.0 (-1.1%)
24	917.0	905.0 (-1.3%)	907.0 (-1.1%)
25	917.0	916.8 (0.0%)	917.7 (0.0%)
26	917.0	916.8 (0.0%)	917.7 (0.0%)
27	917.0	916.9 (0.0%)	917.7 (0.0%)
28	917.0	916.9 (0.0%)	917.7 (0.0%)
29	917.0	916.9 (0.0%)	917.7 (0.0%)
30	917.0	916.9 (0.0%)	917.7 (0.0%)
31	917.0	916.9 (0.0%)	917.7 (0.0%)
32	924.0	916.9 (-0.8%)	917.7 (-0.7%)
33	926.0	916.9 (-1.0%)	917.7 (-0.9%)
34	941.4	939.4 (-0.2%)	922.1 (-2.1%)
35	971.4	999.0 (+2.8%)	981.8 (+1.1%)
36	971.4	999.0 (+2.8%)	981.8 (+1.1%)
37	1058.0	1064.6 (+0.6%)	1053.0 (-0.5%)
38	1058.0	1064.6 (+0.6%)	1053.0 (-0.5%)

Table 4 **Blade lengths (mm) for finite element parameter study of mistuned bladed disks.**

Blade Number	Slightly Mistuned Blade Lengths	Fully Mistuned Blade Lengths
1	92.00001	92.01
2	92.00183	93.83
3	92.00201	94.01
4	92.00127	93.27
5	91.99982	91.82
6	91.99968	91.68
7	91.99960	91.60
8	91.99906	91.06
9	92.00043	92.43
10	92.00046	92.46
11	92.00007	92.07
12	91.99855	90.55

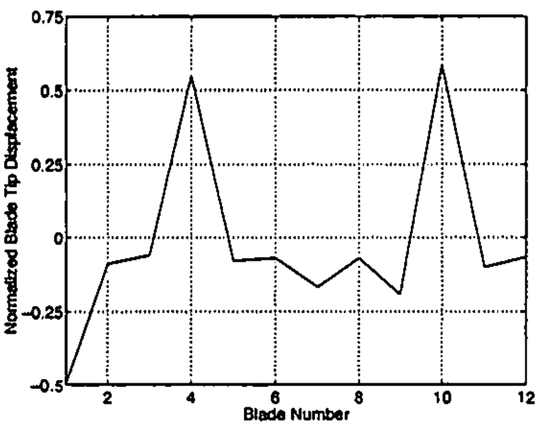

Fig. 9 In-plane blade mode, measured experimentally at 917 Hz for the nominally tuned bladed disk.

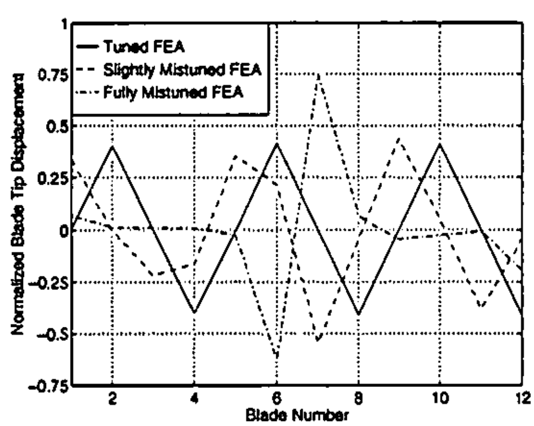

Fig. 10 Effect of blade length mistuning, as predicted by finite element analysis (FEA), on the three nodal diameter in-plane blade mode at 917 Hz.

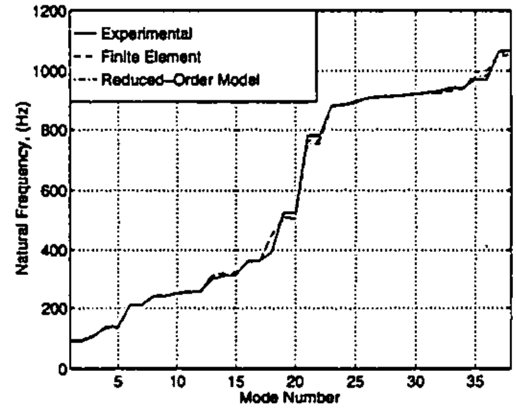

Fig. 11 Natural frequencies for the mistuned bladed disk versus the mode number. Note that the nodal description is no longer a valid manner in which to describe the mistuned mode shapes.

this frequency region cannot be classified according to the nodal diameter description. Clearly, the degradation in the nodal diameter description is much greater for the in-plane blade modes, where there is a high modal density, as opposed to the out-of-plane blade modes, which features only moderate modal density. This observation is consistent with the eigenvalue perturbation result stated earlier.

5. MISTUNED BLADED DISKS AND LOCALIZED MODES

Figure 11 illustrates the correlation between experimental, finite element, and ROM natural frequencies for the mistuned blisk. As demonstrated earlier, the nodal diameter description cannot always be counted on to be an accurate descriptor of bladed disk mode shapes. Therefore, the natural frequencies are plotted versus the mode number, not the number of nodal diameters. Table 5 lists the corresponding natural frequencies along with the percent discrepancy in parenthesis. Note that the repeated root natural frequencies associated with the out-of-plane modes with one nodal diameter (*e.g.*, modes 14 and 15 at 311 and 314 Hz, respectively) split, whereas the repeated root natural frequencies associated with the disk modes (*e.g.*, modes 19 and 20 at 523 Hz) remain extremely close and do not, to an experimentally measurable degree, split. Figure 12 illustrates a mistuned three nodal diameter disk mode at 523 Hz. The effect of mistuning on the nodal diameter description is minimal in comparison to the mode at 311 Hz, shown in Fig. 13. Modes that reside in moderate modal density frequency regions are thus more sensitive to mistuning than the disk modes which are in low modal density regions and whose frequencies do not, to a measurable degree, split.

Figure 14 illustrates the effect of mistuning associated with manufacturing tolerances in the nominally tuned test specimen, and that of additional, deliberate mistuning on the six nodal diameter out-of-plane mode at 256 Hz. Figure 15 illustrates the corresponding correlation between mistuned experimental, finite element, and ROM mode shapes. Clearly, the effect of deliberate mistuning significantly exceeds that of mistuning associated with manufacturing tolerances. The nodal diameter description, although degraded, is still visible in the fully mistuned test specimen.

The in-plane blade modes, by contrast, exhibit significant splitting of the repeated tuned natural frequencies, due to the higher modal density

Table 5 Comparison of experimental, finite element, and ROM mistuned natural frequencies (Hz).

Mode Number	Experimental	Finite Element	Reduced-Order Model
1	88.3	96.0 (+8.7%)	96.5 (+9.3%)
2	90.0	96.4 (+9.2%)	96.6 (+9.4%)
3	107.9	111.0 (+2.9%)	111.5 (+3.3%)
4	141.2	135.0 (-4.4%)	135.8 (-3.8%)
5	141.2	135.1 (-4.3%)	135.8 (-3.8%)
6	211.8	209.2 (-1.2%)	211.4 (-0.2%)
7	211.8	209.2 (-1.2%)	211.7 (0.0%)
8	240.3	239.7 (-0.2%)	242.9 (+1.1%)
9	240.3	241.0 (+0.3%)	243.9 (+1.5%)
10	249.1	250.6 (+0.6%)	253.2 (+1.6%)
11	254.2	254.2 (0.0%)	257.7 (+1.4%)
12	256.0	257.3 (+0.5%)	258.4 (+0.9%)
13	301.4	312.6 (+3.7%)	314.7 (+4.4%)
14	311.2	317.7 (+2.1%)	321.6 (+3.3%)
15	314.5	320.0 (+1.7%)	325.3 (+3.4%)
16	364.0	361.5 (-0.7%)	360.4 (-1.0%)
17	364.0	362.1 (-0.5%)	361.5 (-0.7%)
18	392.5	449.7 (+14.6%)	448.8 (+14.3%)
19	523.0	509.4 (-2.6%)	503.2 (-3.8%)
20	523.0	509.5 (-2.6%)	504.1 (-3.6%)
21	780.0	764.4 (-2.0%)	754.0 (-3.3%)
22	780.0	764.9 (-1.9%)	754.4 (-3.3%)
23	881.9	879.6 (-0.3%)	879.2 (-0.3%)
24	886.0	882.8 (-0.4%)	882.6 (-0.4%)
25	898.0	891.6 (-0.7%)	891.7 (-0.7%)
26	908.0	907.6 (0.0%)	908.2 (0.0%)
27	913.4	909.9 (-0.4%)	910.7 (-0.3%)
28	914.5	911.7 (-0.3%)	912.8 (-0.2%)
29	918.0	915.5 (-0.3%)	916.3 (-0.2%)
30	921.0	921.1 (0.0%)	920.8 (0.0%)
31	927.3	922.9 (-0.5%)	922.1 (-0.6%)
32	932.0	923.8 (-0.9%)	924.9 (-0.8%)
33	943.0	932.6 (-1.1%)	933.7 (-1.0%)
34	943.0	937.7 (-0.6%)	942.3 (-0.1%)
35	970.0	995.5 (+2.6%)	978.5 (+0.9%)
36	970.0	999.6 (+3.1%)	983.1 (+1.4%)
37	1065.3	1059.4 (-0.6%)	1049.3 (-1.5%)
38	1065.3	1065.1 (0.0%)	1054.2 (-1.0%)

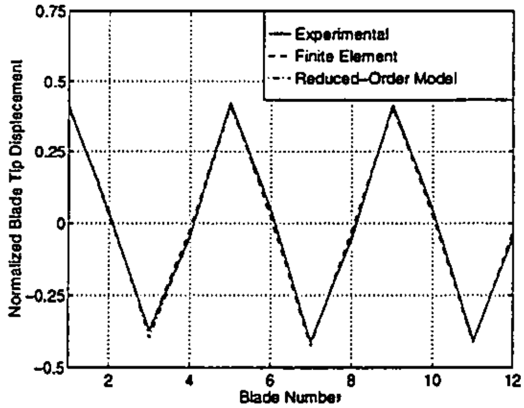

Fig. 12 Comparison of experimental, finite element, and ROM mistuned modes shapes at 523 Hz. Note that disk-dominated modes, which reside in low modal density areas, are largety insensitive to mistuning effects.

associated with these modes—see modes 23 through 31 in Table 5. Figures 16 through 21 illustrate the correlation between experimental, finite element, and ROM in-plane blade modes. Recall that the figures are created by using the absolute value of the blade tip deflection, and hence the modes are extremely localized due to the high modal density in this frequency region. In general, the correlation between experimental, finite element, and ROM modes is excellent. Since vibrational energy is largely concencentrated in a single blade, instead of being spatially extended throughout the structure, there is a strong likelihood that the forced response of the structure to in-plane excitation will greatly exceed the tuned response. The companion paper by Kruse and Pierre (1997) explores this idea further.

6. CONCLUSIONS

Dynamic analysis of turbomachinery rotors has traditionally assumed perfect symmetry among all sectors in the structure. Unfortunately, this assumption imposes spatially extended mode shapes in the structure. The systematic experimental investigation presented in this paper confirms recent computational and analytical findings concerning the confinement of vibration energy to a few, or even a single blade. Mode shapes that are normally assumed to extend throughout the structure were found to localize according to the degree of mistuning and the level of modal density. Out-of-plane blade modes were found to exhibit moderate spatial localization due to mistuning, whereas in-plane blade modes, which are located in dense modal regions, were found to be extremely sensitive to mistuning. It was further demonstrated that both finite element and ROM techniques can accurately predict the onset and extent of localization in bladed disk assemblies. The correlation of the ROM to experimental results is especially beneficial, since both experimental and finite element analyses of mistuned industrial turbomachinery rotors carry a prohibitive cost.

ACKNOWLEDGEMENTS

This work is supported by NASA Lewis Research Center Grant NAG3-1880. Dr. Oral Mehmed is the grant monitor.

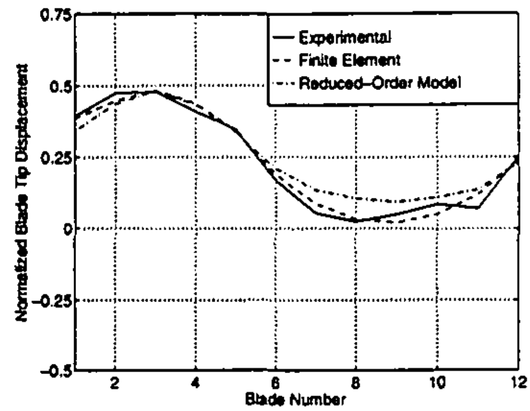

Fig. 13 Comparison of experimental, finite element, and ROM mistuned mode shapes at 311 Hz. Note that out-of-plane blade modes, which reside in moderate modal density areas, are more sensitive to mistuning than disk-dominated modes.

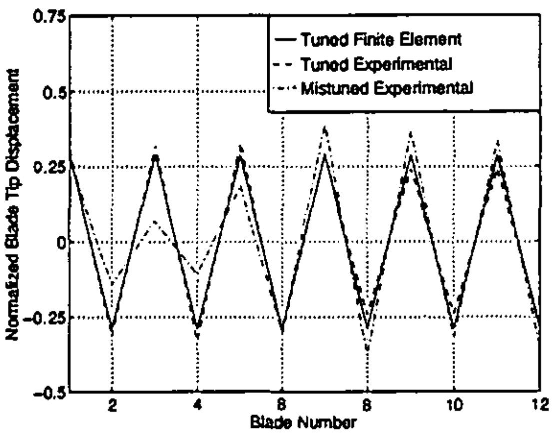

Fig. 14 Comparison of finite element and experimental six nodal diameter tuned modes shapes at 255 Hz with the experimental six nodal diameter mode shape of the mistuned test specimen at 256 Hz.

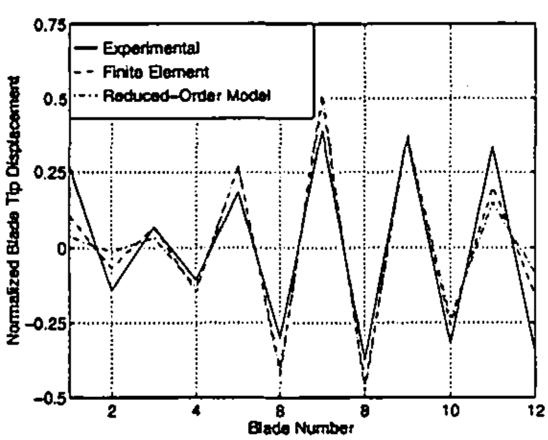

Fig. 15 Comparison of experimental, finite element, and ROM mistuned mode shapes at 256 Hz.

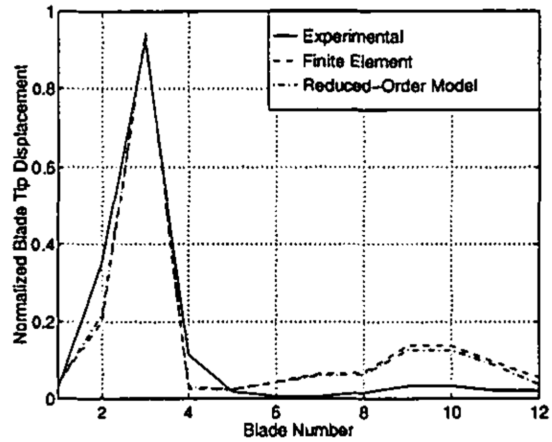

Fig. 16 Comparison of experimental, finite element, and ROM mistuned modes at 882 Hz.

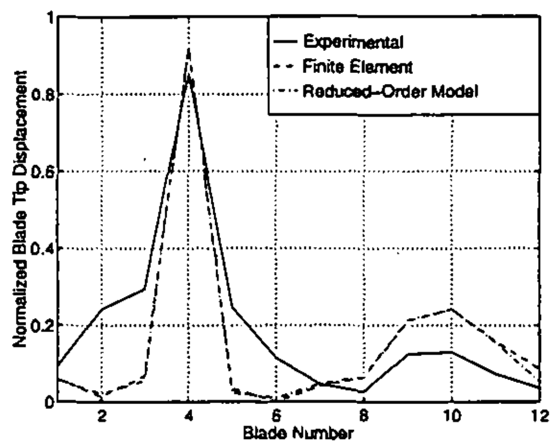

Fig. 17 Comparison of experimental, finite element, and ROM mistuned modes at 898 Hz.

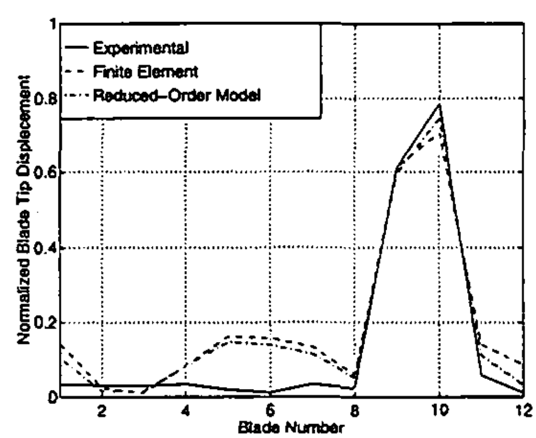

Fig. 18 Comparison of experimental, finite element, and ROM mistuned modes at 908 Hz.

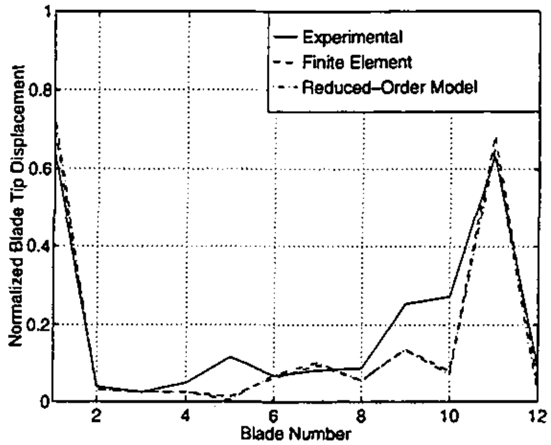

Fig. 19 Comparison of experimental, finite element, and ROM mistuned modes at 918 Hz.

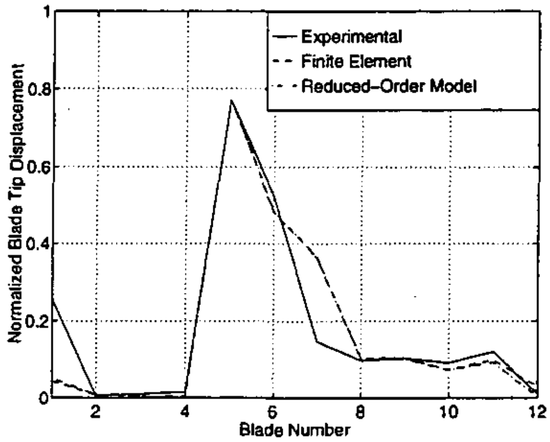

Fig. 20 Comparison of experimental, finite element, and ROM mistuned modes at 921 Hz.

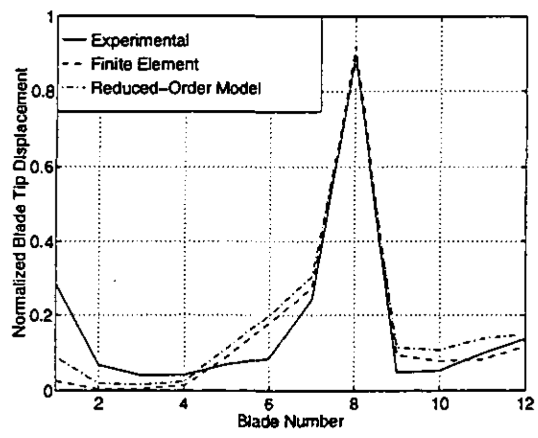

Fig. 21 Comparison of experimental, finite element, and ROM mistuned modes at 932 Hz.

REFERENCES

Ewins, D. J., 1969, "The Effects of Detuning Upon the Forced Vibrations of Bladed Disks," *Journal of Sound and Vibration*, Vol. 9, No. 1, pp. 65–79.

Ewins, D. J., 1973, "Vibration Characteristics of Bladed Disk Assemblies," *Journal Mechanical Engineering Science*, Vol. 15, No. 3, pp. 165–186.

Ewins, D. J., 1976, "Vibration Modes of Mistuned Bladed Disks," *ASME Journal of Engineering for Power*, Vol. 98, No. 3, pp. 349–355.

Fabunmi, J., 1980, "Forced Vibration of a Single Stage Axial Compressor Rotor," *ASME Journal of Engineering for Power*, Vol. 102, No. 2, pp. 322–329.

Irretier, H., 1983, "Spectral Analysis of Mistuned Bladed Disk Assemblies by Component Mode Synthesis," *Proceedings of the Ninth Biennial Conference on Mechanical Vibration and Noise of the Design and Production Engineering Technical Conferences*, pp. 115–125.

Kruse, M. J. and Pierre, C., 1996a, "Dynamic Response of an Industrial Turbomachinery Rotor," *Proceedings of the 32nd AIAA/ASME/SAE/ASEE Joint Propulsion Conference and Exhibit*, Lake Buena Vista, Florida.

Kruse, M. J. and Pierre, C., 1996b, "Forced Response of Mistuned Bladed Disks Using Reduced-Order Modeling," *Proceedings of the 37th AIAA/ASME Strutures, Structural Dynamics, and Materials Conference*, Salt Lake City, Utah.

Kruse, M. J. and Pierre, C., 1997, "An Experimental Investigation of Vibration Localization in Bladed Disks, Part II: Forced Response," *Proceedings of the 42nd ASME Gas Turbine & Aeroengine Congress, User's Symposium & Exposition*, Orlando, Florida.

Ottarsson, G. S., Castanier, M. P., and Pierre, C., 1994, "A Reduced-Order Modeling Technique for Mistuned Bladed Disks," *Proceedings of the 35th AIAA/ASME/ASCE/AHS/ASC Strutures, Structural Dynamics, and Materials Conference*. Also, *ASME Journal of Vibration and Acoustics*, in print.

Pierre, C., 1988, "Mode Localization and Eigenvalue Loci Veering Phenomena in Disordered Structures," *Journal of Sound and Vibration*, Vol. 126, No. 3, pp. 485–502.

Wei, S. T. and Pierre, C., 1988a, "Localization Phenomena in Mistuned Assemblies with Cyclic Symmetry, Part I: Free Vibrations," *ASME Journal of Vibration, Acoustics, Stress, and Reliability in Design*, Vol. 110, No. 4, pp. 429–438.

Wei, S. T. and Pierre, C., 1988b, "Localization Phenomena in Mistuned Assemblies with Cyclic Symmetry, Part II: Forced Vibrations," *ASME Journal of Vibration, Acoustics, Stress, and Reliability in Design*, Vol. 110, No. 4, pp. 439–449.